

# Towards ellipsoidal representations of the gravitational field

Michael Schmidt <sup>a</sup>, Josef Sebera <sup>b,c</sup>, Johannes Bouman <sup>a</sup>, and  
Oliver Fabert <sup>d</sup>,

<sup>a</sup>*Deutsches Geodätisches Forschungsinstitut of the Technische Universität München (DGFI-TUM), Arcisstr. 21, 80333 München, Germany, Email: mg.schmidt@tum.de, johannes.bouman@tum.de*

<sup>b</sup>*Astronomical Institute, Academy of Sciences, Ondřejov, Czech Republic, Email: sebera@asu.cas.cz*

<sup>c</sup>*Research Institute of Geodesy, Cartography and Topography, Zdíby, Czech Republic*

<sup>d</sup>*VU University Amsterdam, Faculty of Sciences, Department of Mathematics, Amsterdam, The Netherlands*

---

## Abstract

The global gravity field of the Earth and other bodies are commonly modelled as series expansions in terms of spherical harmonics which allow an easy computation of the gravitational potential and its functionals. Nevertheless, measured terrestrial and airborne gravity data are usually reduced to a rotating reference ellipsoid, i.e. a spheroid. Thus, oblate ellipsoidal harmonics are much more appropriate than spherical harmonics. Consequently, the computation of the high resolution state-of-the-art combined global gravity field model EGM2008 was performed on the basis of ellipsoidal base functions. The main problem in working with ellipsoidal harmonics, however, is that the evaluation of the associated Legendre functions of the second kind requires the computation of the hypergeometric Gauss functions. In this paper, suitable transformations between ellipsoidal and spherical harmonics are reviewed, as well as renormalization methods that have been developed in the last years. Furthermore, gravity field modelling in terms of spherical (radial) base functions has long been proposed as an alternative to the classical spherical harmonic expansion and is nowadays successfully used in regional or local applications. Here we extend the regional approach and address the multi-resolution representation (MRR) in terms of spheroidal base functions, namely scaling and wavelet functions. The MRR can be applied for both the decomposition of the gravitational field in its spectral components and for the spectral combination of measurements from various observation techniques.

*Key words:* oblate ellipsoidal representation, associated Legendre functions of the second kind, hypergeometric Gauss functions, multi-resolution representation, scaling and wavelet functions

---

## 1 Introduction

The determination and the representation of the gravitational field of the Earth and planetary bodies are some of the most important topics of physical geodesy. In the first-order approximation the Earth is seen as a sphere, whose gravitational force acts in the radial direction from the surface. In geodesy, such fields are commonly approximated with spherical harmonics, which are suitable for processing satellite gravity data acquired from a moderate distance from the Earth. Although new high-accuracy technologies, such as satellite gravity gradiometry, open again the question of the spherical approximation even for satellites (Rummel et al., 2011), the importance of non-spherical methods lies in terrestrial or near-terrestrial (airborne) data processing. For the flattened Earth a spheroidal approximation (in geodesy usually called ellipsoidal), that can be accompanied with spheroidal harmonics, seems to be most appropriate for expressing any quantity located at or near a flattened ellipsoid (Martinec and Grafarend, 1997) and (Grafarend et al., 2006). For example, the geoid height deviates up to 100 m directly about the surface of the reference ellipsoid.

The representation of the gravity field of the Earth in terms of spherical or spheroidal harmonics is only appropriate if the input data are distributed homogeneously over the globe and of similar accuracy. As is evident from the development of EGM2008 (Pavlis et al., 2012) especially terrestrial and airborne measurements are only available in specific regions and are far from being globally distributed. Also radar altimeter measurements do not have a global distribution as they are only given over the oceans. Consequently, the second part of the paper focuses on the inhomogeneous structure of the Earth's gravity field and on the heterogeneous distribution of the input data. The multi-resolution representation (MRR), also known as multi-scale analysis (MSA), is an appropriate candidate for combining measurements from observation techniques of different spatial and spectral resolutions (see e.g. Haagmans et al. (2002)). In the last decades several approaches were pursued to generate a MRR of the gravitational potential by means of spherical (radial) base functions. To be more specific, the application of the wavelet transform allows the decomposition of a given data set into a certain number of frequency-dependent detail signals (see e.g. Freeden et al. (1998), Freeden (1999), Freeden and Michel (2012), Schmidt et al. (2007), Schmidt et al. (2007), Schmidt and Fabert (2008)).

As mentioned before the spheroid means a better approximation of the Earth than a sphere. Consequently, we discuss the basic features of ellipsoidal wavelet

theory to model the Earth's gravitational potential in Section 3. As in the case of ellipsoidal harmonics the associated Legendre functions of second kind have to be computed efficiently for setting up the ellipsoidal scaling and wavelet functions. The paper is concluded with some final remarks in Section 4.

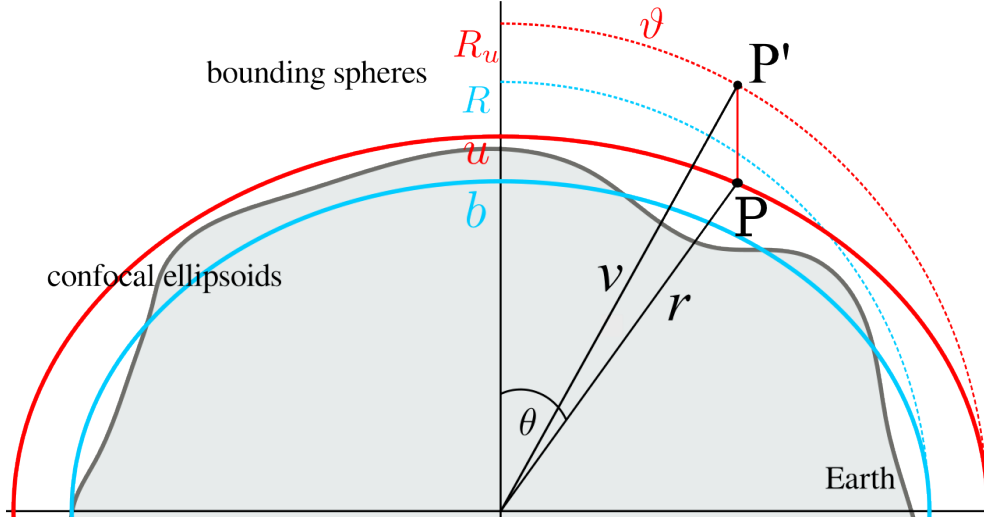


Fig. 1. Definition of spheroidal and spherical coordinates; the origin of the coordinate system coincides with the Earth's center of mass; the radius  $v$  is defined as  $v = \sqrt{u^2 + E^2}$ .

## 2 Global Representations of the Gravitational Potential

We start with Fig. 1 which shows the position of a point  $P$  expressed both with the spherical  $(r, \theta, \lambda)$  and the spheroidal set of coordinates  $(u, \vartheta, \lambda)$ . These two kinds of curvilinear coordinates are related to the geocentric Cartesian coordinates  $(x, y, z)$  by

$$\begin{aligned} x &= \sqrt{u^2 + E^2} \sin \vartheta \cos \lambda = r \sin \theta \cos \lambda, \\ y &= \sqrt{u^2 + E^2} \sin \vartheta \sin \lambda = r \sin \theta \sin \lambda, \\ z &= u \cos \vartheta = r \cos \theta, \end{aligned} \tag{1}$$

where  $r$  and  $u$  are the length of the geocentric radius and the semi-minor axis, respectively,  $E$  is the linear eccentricity with  $E = \sqrt{a^2 - b^2}$  and  $a$  the semi-major axis. The angles  $\theta$  and  $\vartheta$  are the co-latitudes related to the sphere with radius  $r$  through  $P$  and to the sphere bounding the  $u$ -ellipsoid with  $v = \sqrt{u^2 + E^2}$  as shown in Fig. 1. The longitude  $\lambda$  is common for both kinds of coordinates (Thong and Grafarend, 1989).

In these coordinates the Laplace equation  $\Delta V = 0$  can be solved by the separation of variables so that the gravitational potential  $V$  can be expressed with spherical and spheroidal harmonic functions. Generally, the global basis functions are well suited for problems with a global coverage with data. However, for local refinements these global representations can be accompanied with a more localized representation discussed in the Section 3 of this paper.

## 2.1 Spherical Setting

The gravitational potential  $V$  expressed in terms of spherical harmonics reads

$$V(r, \theta, \lambda) = \frac{GM}{R} \sum_{n=0}^{\infty} \sum_{m=0}^n \left(\frac{R}{r}\right)^{n+1} \left(\bar{C}_{n,m}^s \cos m\lambda + \bar{S}_{n,m}^s \sin m\lambda\right) \bar{P}_{n,m}(\cos \theta) \quad (2)$$

(Heiskanen and Moritz, 1967), where  $GM$  denotes the geocentric gravitational constant with the gravitational constant  $G$  and total mass  $M$  of the Earth,  $R$  is the semi-major axis of the reference ellipsoid (or radius of the bounding sphere  $\Omega_R$ ),  $(r, \theta, \lambda)$  is the set of geocentric coordinates, and  $\bar{P}_{n,m}(\cos \theta)$  are the fully normalized associated Legendre function of the 1<sup>st</sup> kind of degree  $n$  and order  $m$ . For numerical investigations we have to replace the infinity symbol ' $\infty$ ' for the summation over  $n$  by a finite value  $n_{\max}$  of the spherical harmonic coefficients  $\bar{C}_{n,m}^s, \bar{S}_{n,m}^s$ . This maximum value governs both the spectral and the spatial resolution of the representation of the potential  $V$ .

Defining the surface spherical harmonics

$$Y_{n,m}(\theta, \lambda) := \bar{P}_{n,|m|}(\cos \theta) \begin{cases} \cos m\lambda & \forall m \geq 0 \\ \sin |m|\lambda & \forall m < 0 \end{cases}, \quad (3)$$

and the coefficients  $V_{n,m}^s := \frac{GM}{R} \cdot \bar{C}_{n,|m|}^s$  for  $m \geq 0$  and  $V_{n,m}^s := \frac{GM}{R} \cdot \bar{S}_{n,|m|}^s$  for  $m < 0$  Eq. (2) can be rewritten in the more compact form

$$V(r, \theta, \lambda) = \sum_{n=0}^{\infty} \sum_{m=-n}^n \left(\frac{R}{r}\right)^{n+1} V_{n,m}^s Y_{n,m}(\theta, \lambda). \quad (4)$$

Introducing the spherical Poisson kernel

$$K^s(r, \theta, \lambda, R, \theta', \lambda') = \sum_{n=0}^{\infty} (2n+1) \left(\frac{R}{r}\right)^{n+1} P_n(\cos \psi) \quad (5)$$

the gravitational potential  $V$  reads

$$V(r, \theta, \lambda) = \frac{1}{S_R} \int_{\Omega_R} K^s(r, \theta, \lambda, R, \theta', \lambda') V(R, \theta', \lambda') d\Omega_R, \quad (6)$$

where  $P_n$  are the Legendre polynomials of degree  $n$  depending on the spherical distance  $\psi$  between the points  $(\theta, \lambda)$  and  $(\theta', \lambda')$  on the unit sphere. In Eq. (6)  $S_R = \text{area}\Omega_R = 4\pi \cdot R^2$  means the total area of the sphere  $\Omega_R$  with radius  $R$  (cf. Fig. 1); the associated surface element  $d\Omega_R$  is given as  $d\Omega_R = R^2 \sin \theta d\theta d\lambda$ . Note, the spherical Poisson kernel (5) can be represented in a closed form (Heiskanen and Moritz, 1967).

## 2.2 Ellipsoidal Setting

Similarly for the oblate ellipsoidal domain, we obtain the spheroidal approximation of  $V$

$$V(u, \vartheta, \lambda) = \frac{GM}{R} \sum_{n=0}^{\infty} \sum_{m=0}^n \frac{Q_{n,m}(i\frac{u}{E})}{Q_{n,m}(i\frac{b}{E})} \left( \overline{C}_{n,m}^e \cos m\lambda + \overline{S}_{n,m}^e \sin m\lambda \right) \overline{P}_{n,m}(\cos \vartheta) \quad (7)$$

(Heiskanen and Moritz, 1967), where  $i^2 = -1$ . The position is given now by the ellipsoidal harmonic coordinates  $(u, \vartheta, \lambda)$  with  $u$  being the semi-minor axis. The  $b$ -ellipsoid, denoted as  $\Sigma_{R,b}$ , and the  $u$ -ellipsoid  $\Sigma_{R,u}$  are con-focal so that they share the same value of the linear eccentricity  $E^2 = R^2 - b^2 = R_u^2 - u^2$ . The attenuation of  $V$  with increasing altitude is now governed by the ratio of the associated Legendre functions of the 2<sup>nd</sup> kind  $Q_{n,m}$ .

As can be seen Eqs. (2) and (7) have nearly the same structure so that a rigorous two-way transformation between  $\overline{C}_{n,m}^e, \overline{S}_{n,m}^e$  and  $\overline{C}_{n,m}^s, \overline{S}_{n,m}^s$  can be formulated. This was first outlined in Hotine (1969) and further developed in Jekeli (1981, 1988). The transformation can be done for all degrees and for a certain degree  $n$  the transformation is defined as a linear combination of lower-degree coefficients. For example for the  $b$ -ellipsoid  $\Sigma_{R,b}$  and the sphere  $\Omega_R$  the transformation reads

$$v_{n,m}^s \Big|_R = \sum_{p=0}^w \frac{\Lambda_{n,m,p} \left( \frac{E}{R} \right)}{\overline{S}_{n-2p,m} \left( \frac{b}{E} \right)} v_{n,m}^e \Big|_b \quad (8)$$

with  $w$  the integer part of  $\frac{n-m}{2}$ , i.e.  $w = \lfloor \frac{n-m}{2} \rfloor$  and

$$\Lambda_{n,m,p} = \frac{(-1)^p (n-p)! (2n-4p+1)!}{p! (n-2p)! (2n-2p+1)!} \left( \frac{E}{R} \right)^{2p} \sqrt{\frac{(2n-4p+1)(n-m)!(n+m)!}{(2n+1)(n-2p-m)!(n-2p+m)!}}$$

where  $\Lambda_{n,m,0} = 1$  for all  $n, m$ . In Eq. (8) the functions  $\overline{S}_{n-2p,m}$  are called Jekeli's functions (Sebera et al., 2012); they are equal to  $Q_{n,m}$  up to additional degree and order functions. Jekeli's functions can be used for both Eq. (7) and Eq. (8) and they are defined as

$$\overline{S}_{n,m} \left( \frac{u}{E} \right) = \frac{\left( \frac{R}{E} \right)^{n+1} i^{n+1} (2n+1)!}{2^n n!} \sqrt{\frac{\epsilon_m}{(2n+1)(n-m)!(n+m)!}} \overline{Q}_{n,m}(z),$$

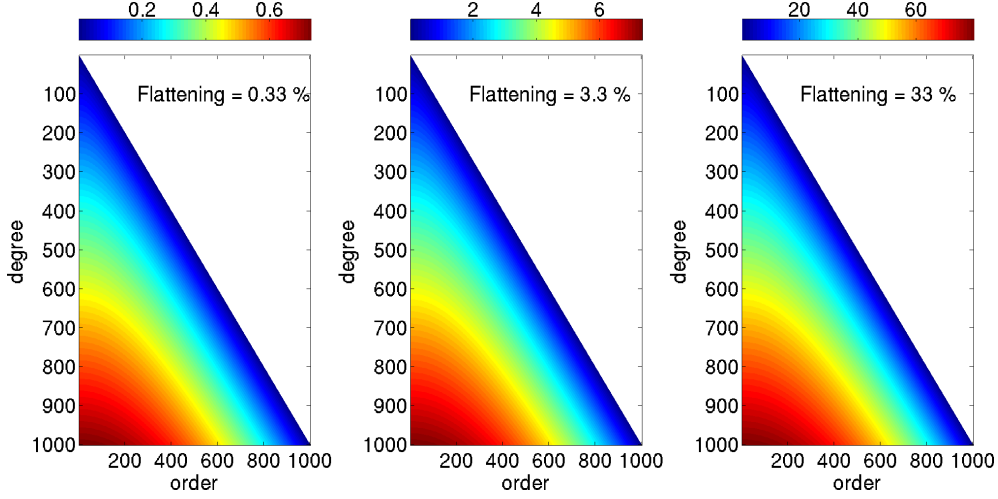


Fig. 2.  $\bar{S}_{n,m}$  functions according to Eq. (11) in  $\log_{10}$  scale for different values of the flattening  $f$  (left panel is for the Earth with  $f = 0.33\%$ ).

where  $\bar{Q}_{n,m} = \sqrt{\frac{(2n+1)(n-m)!}{\epsilon_m(n+m)!}} Q_{n,m}$  (Jekeli, 1988); note, that  $\epsilon_m = 1$  for  $m = 0$  and  $\epsilon_m = 1/2$  for  $m \neq 0$ .

Furthermore, together with the standard definitions of  $Q_{n,m}$  (Hobson, 1931) we can expand Jekeli's function as the hypergeometric series

$$\bar{S}_{n,m} \left( \frac{u}{E} \right) = \left( 1 + \frac{E^2}{u^2} \right)^{\frac{m}{2}} \left( \frac{R}{u} \right)^{n+1} {}_2F_1 \left( \frac{n+m+2}{2}, \frac{n+m+1}{2}, n + \frac{3}{2}, -\frac{E^2}{u^2} \right) \quad (9)$$

(Jekeli, 1988) with the Gauss hypergeometric function  ${}_2F_1$  defined as

$${}_2F_1(\alpha, \beta, \gamma, \delta) = \sum_{k=0}^{\infty} \frac{(\alpha)_k (\beta)_k}{(\gamma)_k} \frac{\delta^k}{k!} \quad (10)$$

(Abramowitz et al., 1965, p. 556), where  $(x)_k = \frac{\Gamma(x+k)}{\Gamma(x)} = \frac{(x+k-1)!}{(x-1)!}$  is the so-called Pochhammer symbol,  $\Gamma$  is the Gamma function and  $k$  means the integer index of the hypergeometric series. How fast the series (10) converges depends on the relative size of the entries  $\alpha, \beta, \gamma$  and  $\delta$ .

Equation (9) can further be optimized for high-degree computations by an appropriate transformation of the hypergeometric series  ${}_2F_1$

$$\bar{S}_{n,m} \left( \frac{u}{E} \right) = \left( \frac{R}{\sqrt{u^2 + E^2}} \right)^{n+1} {}_2F_1 \left( \frac{n+m+1}{2}, \frac{n-m+1}{2}, n + \frac{3}{2}, \frac{E^2}{u^2 + E^2} \right) \quad (11)$$

(Sebera et al., 2015). The function Eq. (11) is plotted in Fig. 2 for three different values of the flattening  $f$ . The left panel holds for  $f = 0.33\%$  close to the flattening of the Earth while the two other panel shows the  $\bar{S}_{n,m}$  for  $f = 3.3\%$  (middle panel) and  $f = 33\%$  (right panel). We see that  $\bar{S}_{n,m}$  has the same appearance for all  $f$  and differs in magnitude only.

As we calculate  $\bar{S}_{n,m}$  via the hypergeometric series, it is useful to see the number of terms involved in the summation (the hypergeometric series is infinite by definition). This is plotted in Fig. 3, where we see that for a relatively low-flattened body and maximum degree 1000 only a few terms are needed (up to 30) to compute  $\bar{S}_{n,m}$  up to numerical precision of  $10^{-16}$ . However, for more flattened bodies many more terms are needed (hundreds) to reach numerical precision, which increases computational costs. For such bodies the recurrences, instead of the hypergeometric formulation, will likely be more advantageous. By comparing the Figs. 2 and 3 one might suspect a close correlation of the magnitude of  $\bar{S}_{n,m}$  with the number of involved terms. Note, however, that this is just a coincidence and not true for other definitions of  $\bar{S}_{n,m}$  (compare with plots in Sebera et al., 2012 that are based on a different form of  $\bar{S}_{n,m}$ ).

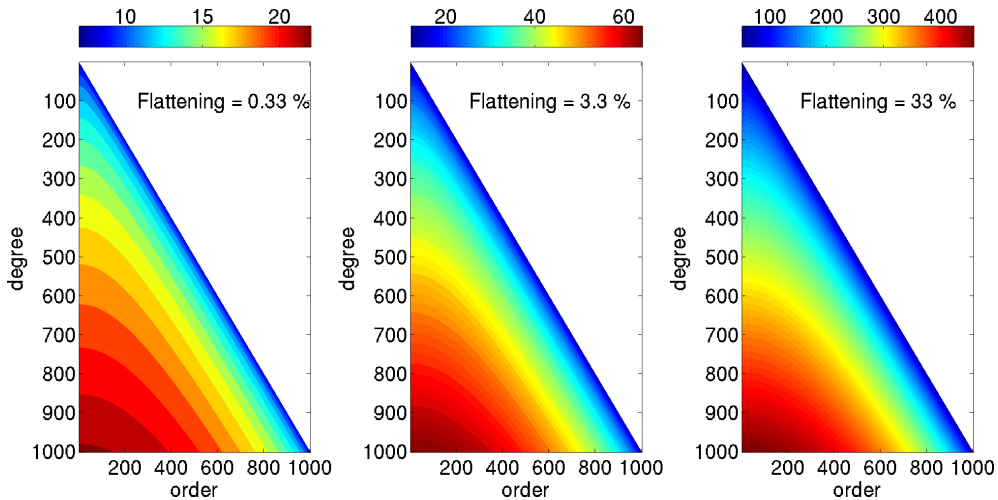


Fig. 3. Number of terms employed in Eq. (10) in order to get  $\bar{S}_{n,m}$  with numerical precision for different values of the flattening (all plots have linear scale).

The Poisson integral equation related to the (reference) ellipsoid  $\Sigma_{R,b}$  with semi-minor axis  $b$  and linear eccentricity  $E = \sqrt{R^2 - b^2}$  as shown in Fig. 1 reads

$$V(u, \vartheta, \lambda) = \frac{1}{S_{R,b}} \int_{\Sigma_{R,b}} K^e(u, \vartheta, \lambda, b, \vartheta', \lambda') V(b, \vartheta', \lambda') d\Sigma_{R,b}, \quad (12)$$

where  $S_{R,b} = \text{area}\Sigma_{R,b} = \frac{2\pi R \cdot b^2}{E} \left( \frac{R \cdot E}{b^2} + \text{arcsinh}\left(\frac{E}{b}\right) \right)$  is the total area of the spheroid  $\Sigma_{R,b}$  and  $d\Sigma_{R,b}$  being the corresponding surface element; see e.g. Schmidt and

Fabert (2008). The ellipsoidal Poisson kernel  $K^e(u, \vartheta, \lambda, b, \vartheta', \lambda')$  is given as

$$K^e(u, \vartheta, \lambda, b, \vartheta', \lambda') = \sum_{n=0}^{\infty} \sum_{m=-n}^n \frac{Q_{n,|m|}\left(\frac{i u}{E}\right)}{Q_{n,|m|}\left(\frac{i b}{E}\right)} Y_{n,m}(\vartheta, \lambda) Y_{n,m}(\vartheta', \lambda') \quad (13)$$

where the surface ellipsoidal harmonics  $Y_{n,m}$  are defined analogously to Eq. (3), but by replacing the spherical coordinates  $\theta$  and  $\lambda$  through the spheroidal coordinate pairs  $(\vartheta, \lambda)$  and  $(\vartheta', \lambda')$ , respectively. As opposed to the spherical Poisson kernel  $K^s$  defined in Eq. (5) the ellipsoidal kernel  $K^e$  depends also on the order values  $m$ ; a closed form is not available.

At the surface of the reference ellipsoid, i.e. for  $u = b$ , the ellipsoidal Poisson kernel reduces under consideration of the addition theorem to

$$K^e(b, \vartheta, \lambda, b, \vartheta', \lambda') = \sum_{n=0}^{\infty} (2n + 1) P_n(\cos \alpha) . \quad (14)$$

As mentioned before in the spherical setting the Legendre polynomial  $P_n$  depends on the spherical distance  $\psi$  between two points on the unit sphere (cf. Eq. (5)). Thus, if we keep one point fixed and vary the other the spherical Poisson kernel  $K^s$  is rotational symmetric, i.e. isotropic. However, for the level ellipsoid  $\Sigma_{R,b}$ , i.e. for Eq. (14), this statement holds only, if the fixed point is the north or the south pole. Consequently, any ellipsoidal kernel is naturally non-isotropic and can be defined as

$$K(u, \vartheta, \lambda, b, \vartheta', \lambda') = \sum_{n=0}^{\infty} \sum_{m=-n}^n \frac{Q_{n,|m|}\left(\frac{i u}{E}\right)}{Q_{n,|m|}\left(\frac{i b}{E}\right)} k_{n,m} Y_{n,m}(\vartheta, \lambda) Y_{n,m}(\vartheta', \lambda') . \quad (15)$$

The degree- and order-dependent coefficients  $k_{n,m}$  define the shape of the kernel; thus, they are called shape coefficients in the following. The dependence of the kernel on the distance  $|u - b|$  is shown in Fig. 4, where it is seen the closer we are to a reference ellipsoid the more terms is needed in Eq. (15).

### 3 Multi-Resolution Representation

The basic idea of the MRR is to split a given input signal into a smoothed approximation and a certain number of band-pass filtered signals by applying a successive low-pass filtering procedure. In the context of wavelet theory, this procedure consists of the decomposition of the signal into scaling and wavelet coefficients and the *(re)construction* of the (modified) signal by means of detail signals. The latter are the spectral components of the MRR because they are related to certain frequency bands. Since we are using sets of basis functions with localizing characteristics the approach presented here can be successfully applied in regional gravity field modelling. For a more detailed description of the method



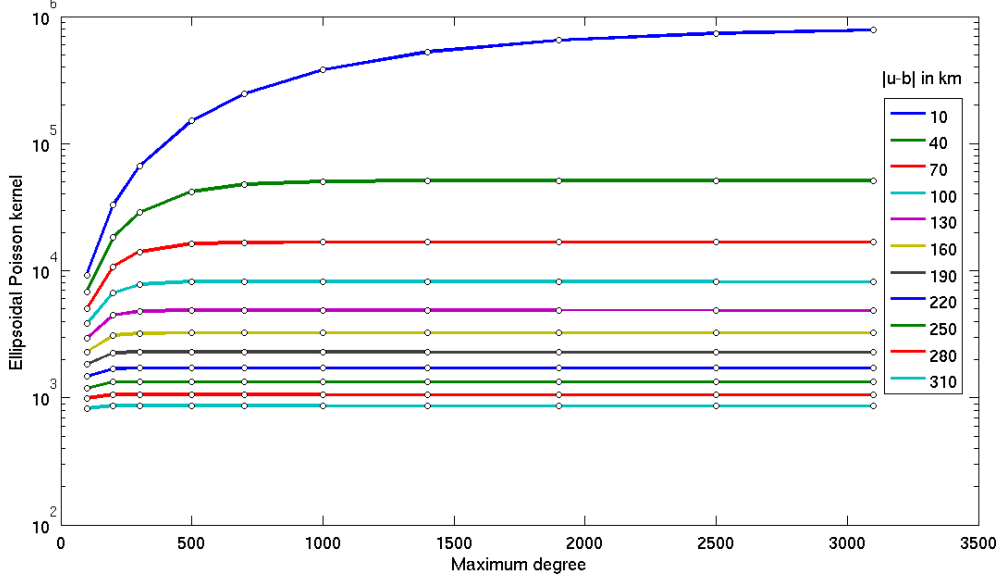


Fig. 4. Convergence of the ellipsoidal Poisson kernel as a function of the  $|u - b|$  and maximum degree.

we refer to [Freeden et al. \(1998\)](#), [Freeden \(1999\)](#), [Freeden and Michel \(2012\)](#), [Schmidt et al. \(2007\)](#), [Schmidt and Fabert \(2008\)](#) and many other publications related to this topic.

According to the wavelet theory we assume that a signal  $F(u, \vartheta, \lambda)$  is given and shall be modelled at the highest level  $J$ . In the context of gravity field modelling we may identify the function  $F(u, \vartheta, \lambda) = V(u, \vartheta, \lambda) - V_{\text{back}}(u, \vartheta, \lambda)$  with the difference of the gravitational potential  $V$  and a given background model  $V_{\text{back}}$  such as EGM2008. Thus, the MRR reads

$$F(u, \vartheta, \lambda) \approx F_{J+1}(u, \vartheta, \lambda) = F_{j'}(u, \vartheta, \lambda) + \sum_{j=j'}^J G_j(u, \vartheta, \lambda) \quad (16)$$

where  $F_{j'}(u, \vartheta, \lambda)$  is the low-pass filtered approximation on level  $j'$ . It can be seen from Fig. 5 that the detail signal  $G_J$  of the highest level  $J$  governs the highest frequencies of the  $F_{j'}(u, \vartheta, \lambda)$ , i.e. it covers the finest structures of the signal under investigation. Mathematically a low-pass filtered signal  $F_{j'}$  and a band-pass filtered detail signal  $G_j$  with  $j \in \{j', \dots, J-1, J, J+1\}$  are computable from

$$F_{j'}(u, \vartheta, \lambda) = \frac{1}{S_{R,b}} \int_{\Sigma_{R,b}} \phi_j(u, \vartheta, \lambda, b, \vartheta', \lambda') F(b, \vartheta', \lambda') d\Sigma_{R,b}, \quad (17)$$

$$G_j(u, \vartheta, \lambda) = \frac{1}{S_{R,b}} \int_{\Sigma_{R,b}} \psi_j(u, \vartheta, \lambda, b, \vartheta', \lambda') F(b, \vartheta', \lambda') d\Sigma_{R,b}, \quad (18)$$

where the level- $j$  scaling function  $\phi_j$  and the level- $j$  wavelet function  $\psi_j$  are defined analogously to Eq. (15) as

$$\phi_j(u, \vartheta, \lambda, b, \vartheta', \lambda') = \sum_{n=0}^{\infty} \sum_{m=-n}^n \frac{Q_{n,|m|}(i\frac{u}{E})}{Q_{n,|m|}(i\frac{b}{E})} \Phi_{j;n,m} Y_{n,m}(\vartheta, \lambda) Y_{n,m}(\vartheta', \lambda'), \quad (19)$$

$$\psi_j(u, \vartheta, \lambda, b, \vartheta', \lambda') = \sum_{n=0}^{\infty} \sum_{m=-n}^n \frac{Q_{n,|m|}(i\frac{u}{E})}{Q_{n,|m|}(i\frac{b}{E})} \Psi_{j;n,m} Y_{n,m}(\vartheta, \lambda) Y_{n,m}(\vartheta', \lambda'). \quad (20)$$

Various relationships exist between the shape coefficients  $\Phi_{j;n,m}$  and  $\Psi_{j;n,m}$  of adjacent levels; see e.g. (Schmidt and Fabert, 2008). As an example we just mention the two-scale relation  $\Psi_{j;n,m} = \Phi_{j+1;n,m} - \Phi_{j;n,m}$ .

In case of band-limited signals the integration over the reference ellipsoid  $\Sigma_{R,b}$

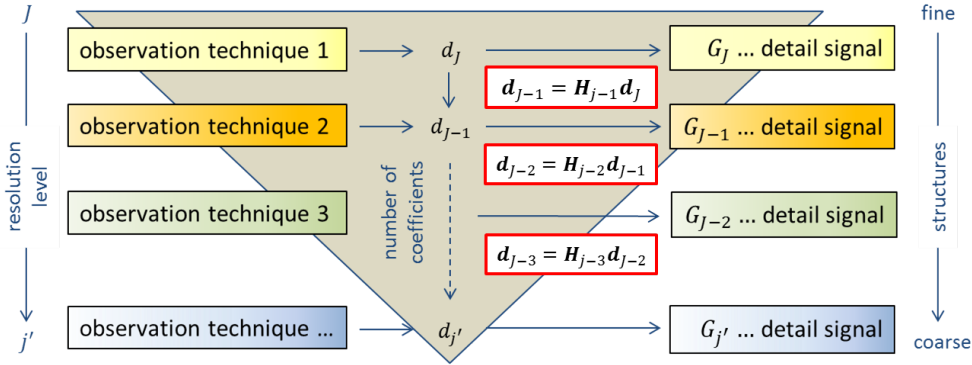


Fig. 5. Concept of a MRR by calculating the detail signals  $G_j$  with  $j = j', \dots, J$  from different observation techniques considering the low pass filter matrices  $H_j$  of the pyramid algorithm.

according to the Eqs. (17) and (18) can be replaced by series expansions in terms of the scaling and wavelet functions  $\phi_j$  and  $\psi_j$  as defined in the Eqs. (19) and (20), respectively. The corresponding series coefficients  $d_{j,k}$  are the basic components of the pyramid algorithm, which relates the coefficients of adjacent levels, e.g. the coefficients  $d_{j,k}$  and  $d_{j-1,l}$  of the two levels  $j$  and  $j - 1$ , respectively, via the low-pass filter matrix  $\mathbf{H}_{j-1}$  as indicated in Fig. 5. Furthermore, we note that (1) the number of series coefficients  $d_{j,k}$  at level  $j$  is twice as large as the number of coefficients  $d_{j-1,l}$  at level  $j - 1$  and (2) the series coefficients  $d_{j-1,l}$  can be transformed into the ellipsoidal harmonic coefficients  $\overline{C}_{n,m}^e, \overline{S}_{n,m}^e$  as introduced in Eq. (7). More details on the procedure addressed before are presented by (Schmidt and Fabert, 2008) and (Schmidt et al., 2015).

Since one of the advantages of the MRR is a regional application directly related to the spectral content of the observation techniques to be combined, the spectral bands  $B_J, B_{J-1}, \dots$  of the highest level values  $J, J - 1, \dots$  are covering very high degree values  $n$ . If we choose, for instance, the highest level  $J$  as  $J = 12$ , which

will be the case in evaluating terrestrial gravity measurements, the corresponding wavelet function  $\psi_{12}$  will cover as a band-pass filter at least the spectral band  $B_{12} = \{n \mid 2048 \leq n < 8192\}$ . Consequently, for numerical computations we replace in Eq. (20) the quotient  $\frac{Q_{n,|m|}(i\frac{u}{E})}{Q_{n,|m|}(i\frac{b}{E})}$  by the quotient  $\frac{\bar{S}_{n,|m|}(i\frac{u}{E})}{\bar{S}_{n,|m|}(i\frac{b}{E})}$  of the Jekeli's functions  $\bar{S}_{n,|m|}$  as defined in the Eq. (11).

We already discussed in the context of Eq. (14) that ellipsoidal kernels are naturally non-isotropic (except at the poles). However, if we assume that the shape coefficients  $\Psi_{j;n,m}$  of the scaling function  $\psi_j$  as defined in Eq. (19) are restricted to

$$\phi_{j;n,m} = \phi_{j;n} \quad \forall \quad n = 0, 1, \dots, \infty, \quad -n \leq m \leq n, \quad (21)$$

they are order-independent and we may benefit from the fact that the computation of the scaling and wavelet functions is drastically simplified as can be seen from the comparison of Eq. (14) with Eq. (15) for  $u = b$ .

For more details concerning these and other scaling and wavelet functions we refer to the textbooks of (Freeden et al., 1998), (Freeden, 1999) and (Freeden and Michel, 2012) as well as to (Schmidt et al., 2007).

#### 4 Final Remarks

From a wide range of approaches for modelling the Earth's gravitational field we presented in this paper two ellipsoidal ones, namely a

- (1) global representation based on ellipsoidal harmonics and a
- (2) regional multi-resolution representation based on ellipsoidal scaling and wavelet functions.

Which of the approaches will be chosen depends on many factors, especially the distribution, the variety and the sensitivity of the input data sets. The presented basis functions, the ellipsoidal harmonics  $Y_{n,m}$ , the ellipsoidal kernel  $K^e$ , or the ellipsoidal scaling and wavelet functions  $\phi_j$  and  $\psi_j$  require all the evaluation of the associated Legendre functions of the 2nd kind. We used the hypergeometric formulation and Jekeli's renormalization for computing the associated Legendre functions. One advantage of this procedure is that the functions  $\bar{S}_{n,|m|}$  from Eq. (11) are also needed for the transformation equation between spherical and ellipsoidal harmonic coefficients defined in Eq. (8).

Finally we want to mention that generally (1) the importance of ellipsoidal approaches rather lies in the analysis (less corrections, continuations is needed etc.), and (2) for users convenience (at least in the global sense) the coefficients are

convertible to the standard spherical coefficients so that a user will not lose his comfort but he can benefit from the ellipsoidal refinements. Since regional refinements depend on global models, e.g. to reduce edge effects (effects from incomplete domain, long wavelengths etc.) regional and global model approaches should be developed as complementary tools.

## References

- Abramowitz, M., Stegun, I. A., et al. (1965). *Handbook of mathematical functions*, volume 1046. Dover New York.
- Freedon, W. (1999). *Multiscale modelling of spaceborne geodata*. Teubner.
- Freedon, W., Gervens, T., and Schreiner, M. (1998). *Constructive approximation on the sphere with applications to geomathematics*. Oxford University Press on Demand.
- Freedon, W. and Michel, V. (2012). *Multiscale potential theory: with applications to geoscience*. Springer Science & Business Media.
- Grafarend, E., Finn, G., and Ardalan, A. (2006). Ellipsoidal vertical deflections and ellipsoidal gravity disturbance: case studies. *Studia Geophysica et Geodaetica*, 50(1):1–57.
- Haagmans, R., Prijatna, K., and Omang, O. D. (2002). An alternative concept for validation of GOCE gradiometry results based on regional gravity. *Earth*, 1(1):1.
- Heiskanen, W. A. and Moritz, H. (1967). *Physical geodesy*. W. H. Freeman and Company, San Francisco.
- Hobson, E. W. (1931). *The theory of spherical and ellipsoidal harmonics*. Cambridge, Great Britain.
- Hotine, M. (1969). *Mathematical geodesy*. ESSA, U.S. Department of Commerce.
- Jekeli, C. (1981). The downward continuation to the Earth’s surface of truncated spherical and ellipsoidal harmonic series of the gravity and height anomalies. Technical Report 323, Ohio State University.
- Jekeli, C. (1988). The exact transformation between ellipsoidal and spherical expansions. *Manuscripta geodaetica*, 13:106–113.
- Martinec, Z. and Grafarend, E. W. (1997). Solution to the Stokes boundary-value problem on an ellipsoid of revolution. *Studia Geophysica et Geodaetica*, 41:103–129.
- Pavlis, N. K., Holmes, S. A., Kenyon, S., and Faktor, J. K. (2012). The development and evaluation of the earth gravitational model 2008 (egm2008). volume 117, page B04406.
- Rummel, R., Yi, W., and Stummer, C. (2011). GOCE gravitational gradiometry. *Journal of Geodesy*, 85:777–790. 10.1007/s00190-011-0500-0.
- Schmidt, M. and Fabert, O. (2008). Ellipsoidal Wavelet Representation of the Gravity Field. *OSU report*, 487.

- Schmidt, M., Fengler, M., Mayer-Gürr, T., Eicker, A., Kusche, J., Sánchez, L., and Han, S.-C. (2007). Regional gravity modeling in terms of spherical base functions. *Journal of Geodesy*, 81(1):17–38.
- Schmidt, M., Göttl, F., and Heinkelmann, R. (2015). Towards the Combination of Data Sets from Various Observation Techniques. In: Kutterer et. al.: The 1st International Workshop on the Quality of Geodetic Observation and Monitoring Systems (QuGOMS'11). *Proceeding of the 2011 IAG International Workshop*, 140.
- Sebera, J., Bezděk, A., Kostelecký, J., Pešek, I., and Shum, C. (2015). An ellipsoidal approach to update a high-resolution geopotential model over the oceans: study case of EGM2008 and DTU10. *Advances in Space Research*, (under review).
- Sebera, J., Bouman, J., and Bosch, W. (2012). On computing ellipsoidal harmonics using Jekeli's renormalization. *Journal of Geodesy*, pages 1–14. 10.1007/s00190-012-0549-4.
- Thong, N. and Grafarend, E. (1989). A spheroidal harmonic model of the terrestrial gravitational field. *Manuscr. Geod.*, 14:285–304.